

Evaluation and Correction Analysis of the Regional Rainfall Simulation by CMIP6 over Sudan

Waleed Babiker^{A,B,C}, Guirong Tan^{A*}, Mohamed Abdallah Ahmed Alriah^{C,D,E}, Ayman M. Elameen^{E,F}

^A School of Atmospheric Sciences, Nanjing University of Information Science and Technology, Nanjing 210044, China; waleedbab200@gmail.com, tanguirong@nuist.edu.cn

^B Environmental Protection Department, Air Quality and Meteorology, Aramco Saudi Arabia, P.O. Box 5000, Dhahran 31311, Kingdom of Saudi Arabia

^C Sudan Meteorological Authority, Khartoum - P.O. Box 574, Sudan; mabdallah318@yahoo.com

^D School of Geographical Sciences, Nanjing University of Information Science and Technology, Nanjing 210044, China

^E Organization of African Academic Doctors (OAAD), Nairobi, Kenya; aymanmohamed1991@outlook.com

^F School of Remote Sensing and Geomatics Engineering, Nanjing University of Information Science and Technology, Nanjing 210044, China

KEYWORDS

Sudan
CMIP6
rainfall
GCM evaluation
bias correction

ABSTRACT

This study utilizes satellite-based rainfall CHIRPS to evaluate GCMs-CMIP6 models over Sudan from 1985 to 2014. Overall, the GCMs of BCC-CSM2-MR, CAMS-CSM1-0, CESM2, EC-Earth3-Veg, GFDL-ESM4, MIROC-ES2L, and NorESM2-MM are well reproduced in the unimodal pattern of June to September (JJAS), and hence employed to calculate Multi-Model Ensemble (MME). Then, we examine the capability of the GCMs and MME in replicating the precipitation patterns on annual and seasonal scales over Sudan using numerous ranking metrics, including Pearson Correlation Coefficient (CC), Standard Deviation (SD), Taylor Skill Score (TSS), Mean Absolute Error (MAE), absolute bias (BIAS), and, normalized mean root square error (RMSD). The results show that the MME has the lowest bias and slightly overestimates rainfall over most parts of our study domain, whilst, others (ACCESS-CM2, BCC-CSM2-MR, CAMS-CSM1-0, CESM2, CNRM-CM6-1, CNRM-CM6-1-HR, CNRM-ESM2-1, FGOALS-f3-L, FGOALS-g3) consistently overestimate rainfall in referring to CHIRPS data, respectively, but FIO-ESM-2-0 underestimates bias value. Moreover, MIROC-ES2L and NorESM2-MM demonstrate better performance than the other models. Finally, we employed a bias correction (BC) technique, namely Delta BC, to adjust the GCMs model products through the annual and monsoon seasons. The applied bias correction technique revealed remarkable improvement in the GCMs against the observations, with an improvement of 0–18% over the original. However, MME and MIROC-ES2L show better performance after correction than other models.

* Corresponding author: Guirong Tan: tanguirong@nuist.edu.cn

doi: 10.5937/gp28-46565

Received: September 15, 2023 | Revised: February 14, 2024 | Accepted: March 21, 2024

Introduction

Africa is the second-populated continent in the world, with a population of 1.2 billion and an area of about 30 million km² (11.6 million mi²), and one of the most vulnerable to climate change due to its high exposure to droughts, floods, rising temperatures with little ability to adapt (Almazroui et al., 2020). However, Sudan, which lies in the eastern part of the continent, is considered one of the most vulnerable countries to the risks of climate change, especially flood and drought (Alhuseen, 2014), and has experienced several environmental changes in the past, and more are projected to occur in the future (Walthall, 2012). The implementation of the United Nations Framework Convention on Climate Change (UNFCCC), with several studies, shows that the development process will be greatly impacted by climate change, especially in fields like water, agriculture, and health (Alhuseen, 2014).

To investigate the present and future of Earth's climate system, many global climate models have been developed (Kumar et al., 2013). Furthermore, future changes in rainfall across this region must be detected and understood by stakeholders in resource management and planning, as the variability of the future climate is a major concern (Rajbhandari, et al., 2018). Since the primary tools of the analyses and determining what climate we are likely to have in the near and not-so-near future use dynamical downscaling with regional climate models (RCMs) and global climate models (GCMs) (Maroneze et al., 2014), the evaluation of climate models is considered as essential for providing model-based climate data (Babaousmail et al., 2022). Several climate modeling organizations have run climate simulations for the future using various IPCC emission scenarios (Rajbhandari et al., 2018). Global climate models (GCMs), which are mostly used for continental and hemispherical climate research, have proven to be a useful tool for analyzing the changes that could have an impact on these systems in the future. However, due to their typical spatial resolutions, which are on the order of hundreds of kilometers (Expósito et al., 2015), furthermore, often, the availability of numerous GCMs is seen as the main cause of uncertainty in precipitation projections (Tegegne & Mellese, 2022). So, it is critical to evaluate the fundamental uncertainty. The interior variability of the climate system, model error, and uncertainty in the greenhouse emission scenario are three potential causes of uncertainty in climate projections (Ishida et al., 2020). Therefore, our results should be reduced to a more accurate resolution to reliably evaluate the regional effects

of climate change (Ishida et al., 2020). The model evaluation for this study was based on a range of statistical measurements and visual graphical comparisons for the same aggregation periods to postulate potential changes in precipitation (Akurut et al., 2014). These are generally three-dimensional dynamic and physical models of the atmosphere, ocean, Earth's surface, and cryosphere that are coupled and run on supercomputers at full power. Around the world, there are many models of this type, all with varying formulations, strengths, and weaknesses, leading to one of the main uncertainties in climate change projections (Collins & Senior, 2002).

This insight is particularly important in climate research on Sudan's complex orography, where regional models should be able to resolve a few kilometers. The attribution of uncertainties in the projection study brings to light some factors, such as systematic and non-systematic biases in the model datasets or methods that take into account the natural variability of the climate, such as the El Nino-Southern oscillation or warming of the tropical oceans (Ngoma et al., 2021). Hence, from the perspective of climate dynamics, the spatial and temporal variability of precipitation poses a variety of difficulties for process comprehension, event prediction, and climate change projection, and the urgency of the issue is increased by the fact that many communities in Africa are particularly vulnerable to climate change (Badr et al., 2016). Also, the rainy season for this study, which spans from June to September over the entire region, was linked to the annual migration of the intertropical convergence zone (ITCZ), where the Atlantic Ocean, Red Sea, Mediterranean, and Indian Ocean are the major main sources of water vapor (Salih et al., 2015). The variability of rainfall in various locations in Sudan is significantly influenced by sea surface temperature (SST) in the Indian and Pacific Oceans, and the Atlantic Multidecadal Oscillation (AMO) is brought on by modifications in essence.

Based on the aforementioned studies, and to address the gap in existing research in this area, as far as we know, we seek to conduct such a study. This study aims to evaluate the performance of a general circulation model (GCM) in simulating regional rainfall and to correct any potential biases through data assimilation techniques. The study aims to assess the accuracy of the GCM simulations by comparing them against the Climate Hazard Group Infrared Precipitation with Station (CHIRPS) dataset over Sudan and to identify any discrepancies or biases in the model.

Materials and Methods

Study area

Sudan is situated in Eastern Africa within [8.4 and 23.3° N] and [21.5 and 39.0° E] as in (Figure 1). Its total area is 1,886,068 km², with adjoint borders with South Sudan from the South, Ethiopia and Eritrea in the East, Libya Northwest, Chad and Central Africa in the West, and Egypt in the North (Elramlawi et al., 2018).

Arabian Peninsula that were blowing North and advverting moisture from the Red Sea. August, is the wettest month of the year in much of Sudan, with up to 100 mm/month (Alriah et al., 2021). However, there is a humid area on the Red Sea coast, where the rains fall during the winter with a sporadic distribution with a peak quantity in November, and also fall during the summer when the tem-

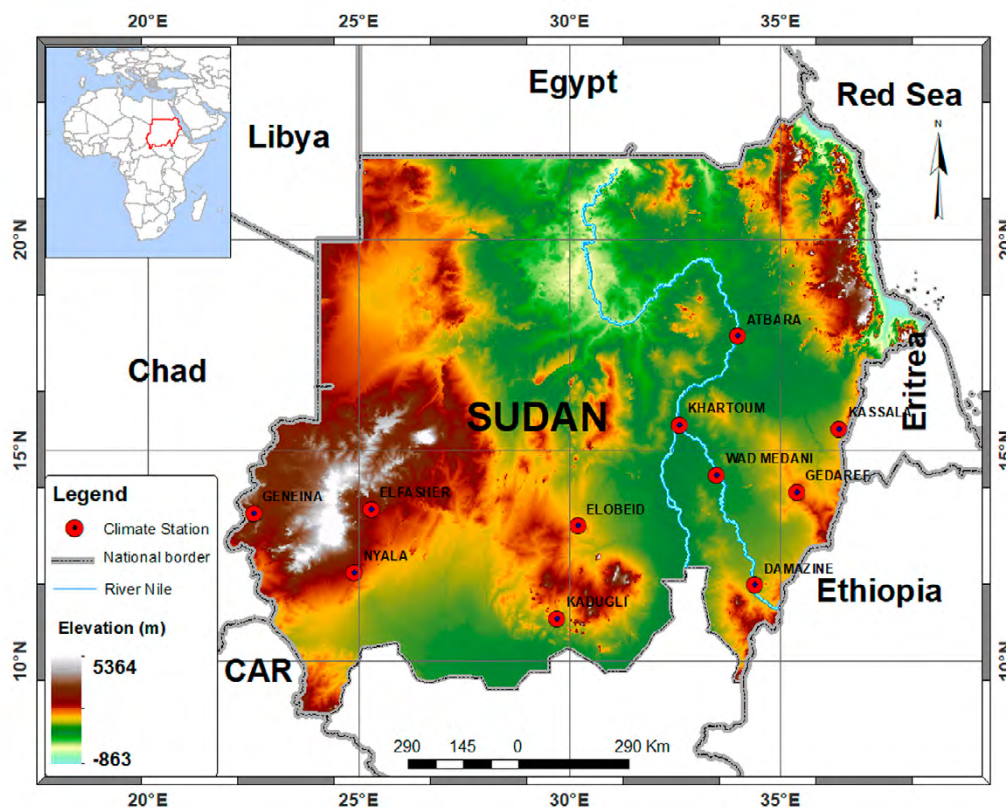


Figure 1. The study area location and its topographical features

Rainfed agriculture inhabits more than 90% of the cultivated land, producing agricultural products and the related means of subsistence for the Sudanese people (Siddig et al., 2020). The country is characterized by several topographic features such as the valleys of the Blue and White Nile Rivers, and the elevated eastern and southern boundaries, as well as the main Nile River and its tributaries, besides some isolated uplands (Williams & Nottage, 2006). The dry season in the country spans from October to March, followed by a hot season from April to June, and a wet season from June to September. However, the environment and social circumstances in Sudan are significantly influenced by rainfall (Gamri, et al., 2009). The rainy season (June to September) across Sudan has been linked to the annual migration of the Intertropical Convergence Zone (ITCZ) (Salih et al., 2015). During the boreal summer, this rainfall was brought on by winds from the

perature is moderate. In other locations, August is typically the month with the most rainfall, but July can also be rainy in some places, from one region to another, there is a significant difference in the quantity of rainfall and the length of the rainy season (Ahmed & Elhag, 2011).

Data

This study used Climate Hazard Group Infrared Precipitation with Station monthly precipitation datasets (CHIRPS. v2), with a spatial resolution 0.05° × 0.05° (5.55 x 5.55 km²) (<https://data.chc.ucsb.edu/products/CHIRPS-2.0/>), was obtained from (1985-2014), it is blending station data and reduce any uncertainties that may lack rain gauge, therefore, it has a better performance among east Africa and recently evaluated over the study domain (Alriah et al., 2022).

Also, the initial realizations (r1i1p1f1), for all CMIP6 models were downloaded from the website (<https://>

Table 1. The GCMs-CMIP6 information and their spatial coverage

Nº	Model ID	Country	resolution	Reference
1	ACCESS-CM2	Australia	1.9° × 1.3°	(Mkala et al., 2023)
2	BCC-CSM2-MR	China	1.1° × 1.1°	(Wu et al., 2021)
3	CAMS-CSM1-0	China	1.1° × 1.1°	(S & L, 2023)
4	CESM2	USA	1.3° × 0.9°	(Meehl et al., 2020)
5	CNRM-CM6-1	France	1.4° × 1.4°	(Voldoire et al., 2019)
6	CNRM-CM6-1-HR	France	0.5° × 0.5°	(Weijer et al., 2020)
7	CNRM-ESM2-1	France	1.4° × 1.4°	(Séférian et al., 2019)
8	EC-Earth3-Veg	Europe	0.7° × 0.7°	(Babaousmail et al., 2021)
9	FGOALS-f3-L	China	1.3° × 1°	(Klutse et al., 2021)
10	FGOALS-g3	China	2° × 2.3°	(Wang et al., 2022)
11	FIO-ESM-2-0	China	1.3° × 0.9°	(Bao et al., 2020)
12	GFDL-ESM4	USA	1.3° × 1°	(Zheng et al., 2022)
13	MIROC-ES2L	Japan	2.8° × 2.8	(Hajima et al., 2020)
14	MRI-ESM2-0	Japan	1.1° × 1.1°	(Kawai et al., 2019)
15	NorCPM1	Norway	1.9° × 2.5°	(Bethke et al., 2021)
16	NorESM2-MM	Norway	1.3° × 0.9°	(Seland et al., 2020)

cds.climate.copernicus.eu/cdsapp#!/dataset/projections-cmip6). Climate models' information and details of the 16 historical GCM models utilized in this study are obtained in Table 1.

Methodology

The evaluation of climate models is a critical step in assessing the accuracy and reliability of their outputs. Hence, the best correlated methods are selected based on statistical and error measures like the Pearson Correlation Coefficient (CC), Standard Deviation (SD), Taylor Skill Score, Mean Absolute Error (MAE), and absolute bias (BIAS). Many scholars, (Alriah et al., 2022; Karim et al., 2023), use it for comparing the performance of the climate data simulation against the observed data using the climatology of annual and intra-annual time scales. Here, we used a multi-Models ensemble for the best selected GCM models, after unifying (Bilinear-interpolation) their resolution into the same resolution of reference data (CHIRPS), followed by averaging the CHIRPS dataset within the region, as shown in the equations below.

$$M\bar{x} = \frac{1}{n} \sum_{i=1}^n x_i \quad (1)$$

The variability is calculated using the Square Root of Variance (standard deviation), represented as σ ,

$$\sigma_x = \sqrt{\frac{1}{n} \sum_{i=1}^n (x_i - \bar{x})^2} \quad (2)$$

Where x_i is the monthly rainfall, \bar{x} is the mean of the entire series, and σ_x is the standard deviation for the models, with respect to data used to rate the evaluation. Furthermore, the measure of statistical error validation of model-based versus observed-based precipitation.

$$CC = \frac{\sum_{n=1}^n (G_i - \bar{G})(S_i - \bar{S})}{\sum_{n=1}^n (G_i - \bar{G})^2 \sum_{n=1}^n (S_i - \bar{S})^2} \quad (3)$$

It was used to evaluate the observation data and dataset of the gridded simulation model, when the CC is close or equal to 1, it means that there is a correlate high, the negative bias expresses the area where the model is higher than the reference data, and positive bias expresses the area the model is lower than the observation data.

$$TSS = \frac{4(1 + R_m)^2}{\left(\frac{\sigma_m + \sigma_o}{\sigma_o - \sigma_m}\right)^2 (1 + R_o)^2} \quad (4)$$

For both models and observation patterns, R_m is the correlation coefficient, and R_o is the maximum possible correlation coefficient (i.e., 0.999), whereas m and o are the standard discrepancies from the simulation and reference precipitation patterns, respectively. Between 0 and 1, the TSS value is measured, with values closer to 1 indicating higher model performance.

$$BIAS = \frac{\sum_{i=1}^n G_i - S_i}{\sum_{i=1}^n G_i} \quad (5)$$

In order to evaluate the model, we calculate the Mean Bias of GCM- The difference between the observed and modeled rainfall is calculated to determine the mean bias. The mean bias is calculated for monthly rainfall based on the CHIRPS dataset, the GCM and the observations to obtain a spatial distribution of the mean bias, Overall, spatial distribution of mean bias GCM of rainfall is a crucial step to determine the accuracy and reliability of GCM simulations, and it helps to suggest improvements in the GCM models. Climate Index: In order to evaluate the climate model with reference data (CHIRPS) the large-scale effects of atmospheric circulation on rainfall. This bias can be due to a variety of factors, such

as inaccuracies in the models’ physical processes, limitations in the models’ spatial or temporal resolution, or errors in the input data used to initialize and run the models. The framework process of this study is illustrated in the flowchart (Figure 2).

For precipitation variables, the bias in a geographical location x is given by the difference between observed and simulated precipitation, Bias-corrected precipitation in x at some time t in the past was estimated as below (Mendez et al., 2020).

$$P_{ass}^{BC} = \frac{Pass(d) \cdot \left[\frac{\mu_m(P_{obs(t)})}{\mu_m(P_{ass(t)})} \right]}{30} \quad (6)$$

Where a simulation historical of precipitation GCM to be corrected, reference observation precipitation CHIRPS dataset, a simulation historical of precipitation GCM.

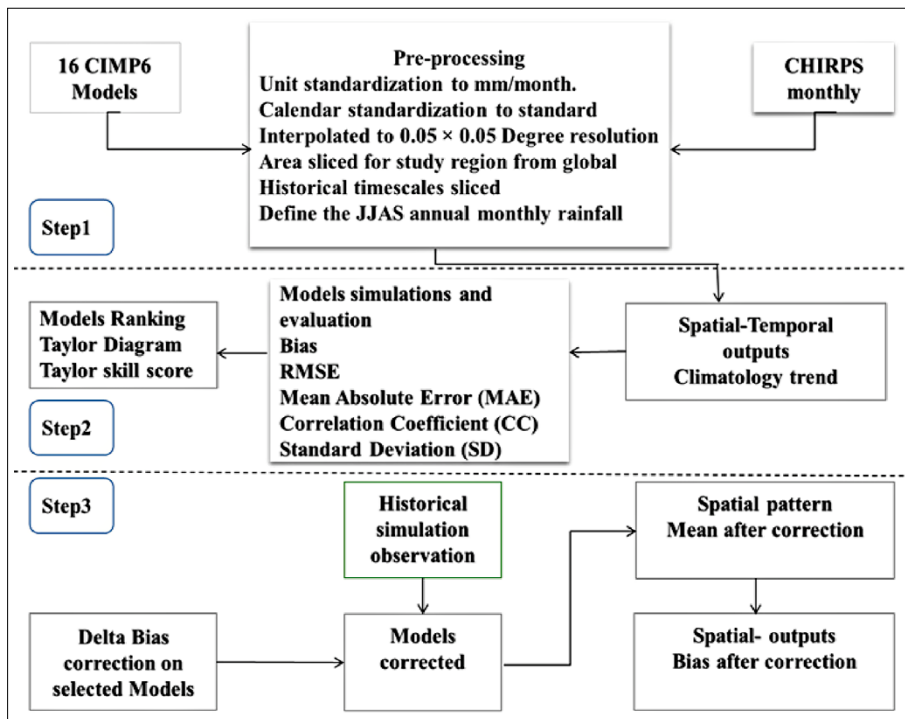


Figure 2. The framework of this study is presented in a flow-chart format for historical data processing, evaluation, and Bias correction, of rainfall variables over the study Domain

Results

Climatology of Rainfall

The rainfall of Sudan is heavily influenced by the Inter-Tropical Convergence Zone (ITCZ). Hence, the country experiences a variety of summer rainy seasons from June to September. The region’s diverse topography also affects where and how much rainfalls, with the South-

east and Southwest zones receiving more rain than the Northern zone. Figure 3 shows the monthly mean rainfall time series of CHIRPS and 16 GCMs over Sudan during 1985 - 2014. We compare the GCMs products against the reference data (CHIRPS) based on the annual cycle to see how well the models could represent the observed pre-

precipitation pattern. The degree to which a model can properly mimic precipitation is what determines how accurate it is. The GCMs' monthly precipitation trends demonstrate distinct patterns that represent the annual mean precipitation cycle in our domain. Most of the models exhibit a unimodal peak in August; however, few models show a bimodal peak in June and September. The rainfall amounts vary from 0 to 105 mm/month across the models, with relatively higher rainfall amounts during the peak months. The following models: BCC-CSM2-MR, CAMS-CSM1-0, CESM2, EC-Earth3-Veg, GFDL-ESM4, MIROC-ES2L, and NorESM2-MM robustly replicate the peak rainfall while reproducing different rainfall amounts. They also have a shallow bias, which means that they simulate a lower range of precipitation values than the reference data. However, it might suggest that averaging a group of different GCMs that perform well may result in better rainfall simulation than using a single GCM. Therefore, these seven advantageous GCMs were averaged as mean ensemble model (MME) and examined alongside the other 16 GCMs in the following analyses. The obtained results further revealed that the ACCESS-CM2, FGOALS-f3-L, FGOALS-g3, CNRM-CM6-1, CNRM-CM6-1-HR, and CNRM-ESM2-1 are notably underestimating the mean rainfall.

Specifically, the CNRM-CM6-1, CNRM-CM6-1-HR, and CNRM-ESM2-1 are found to be strongly underestimating the precipitation than other GCMs. The models observed

to underestimate precipitation may have insufficient representation of the atmospheric and oceanic processes that contribute to our study domain. On the other hand, FIO-ESM2-0 was detected to be significantly overestimating the mean of precipitation. Overall, the models that significantly underestimate or overestimate precipitation may have inaccurate parameterizations, which could lead to erroneous projections of future water availability, and thus, have serious consequences for the country's agricultural and economic sectors. In conclusion, the GCMs showed varying levels of skill in simulating the Sudan rainfall regime. The accuracy of the GCMs in simulating precipitation over Sudan has significant implications for climate change projections and regional water resource management; therefore, further investigation and improvement are required.

Model performance evaluation

Here, the performance of the considered CIMP6 models for this study is evaluated against the CHIRPS dataset to assess their capabilities in simulating annual and seasonal (JJAS) rainfall over Sudan from 1985-2014. Numerous validation metrics including Pearson's correlation coefficient (CC), standard deviation (SD), Taylor Skill Score (TSS), Mean Absolute Error (MAE), and absolute bias (BIAS) are employed to evaluate and test the model's performance versus CHIRPS observation. Taylor diagrams for annu-

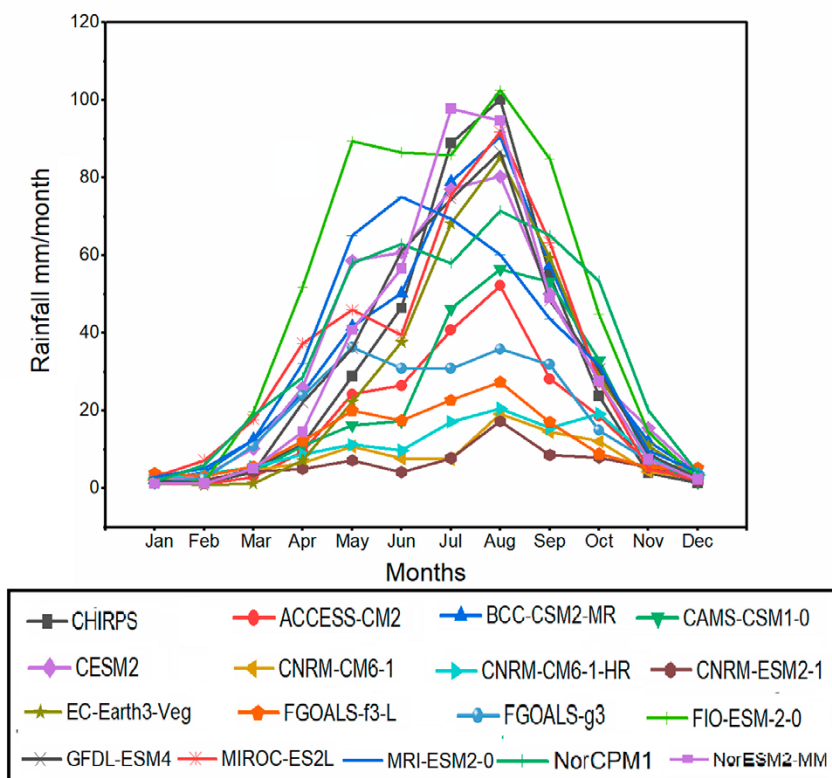


Figure 3. Monthly mean rainfall of CHIRPS and 16 multi-model ensembles (mm/month), the black line is the reference dataset (CHIRPS)

al and seasonal comparison are shown in Figures 4 and 5, whilst the values of TSS and BIAS are illustrated in Figures 6 and 7, respectively. Tables 2 and 3 summarize the outcomes of the previous statistical metrics during the annual and seasonal (JJAS) comparisons. It found that all GCMs produced higher scores in terms of TSS, CC, MAE, RMSD, and BIAS during annual comparisons than seasonal (JJAS) comparisons. This result indicates that those models simulate the rainfall over Sudan during the annual phase more accurately than the seasonal (JJAS) phase. Moreover, through the annual comparison, the MME cap-

tured the largest score in terms of TSS, CC, MAE, RMSD, and BIAS with values of 93%, 96%, 6.76, 10.37, and 0.42, respectively. On the other side, CESM2 captured the highest score in terms of TSS, MAE, and RMSE during the seasonal (JJAS) comparison and showed reads of 50%, 8.8, and 10.5, respectively, while CAMS-CSM1-0 demonstrated the highest CC (41%) and NorESM2-MM showed the lowest bias (-0.42).

Our results further showed that the following models: NorESM2-MM, EC-Earth3-Veg, GFDL-ESM4, BCC-CSM2-MR, MIROC-ES2L, and CESM2 outperform the

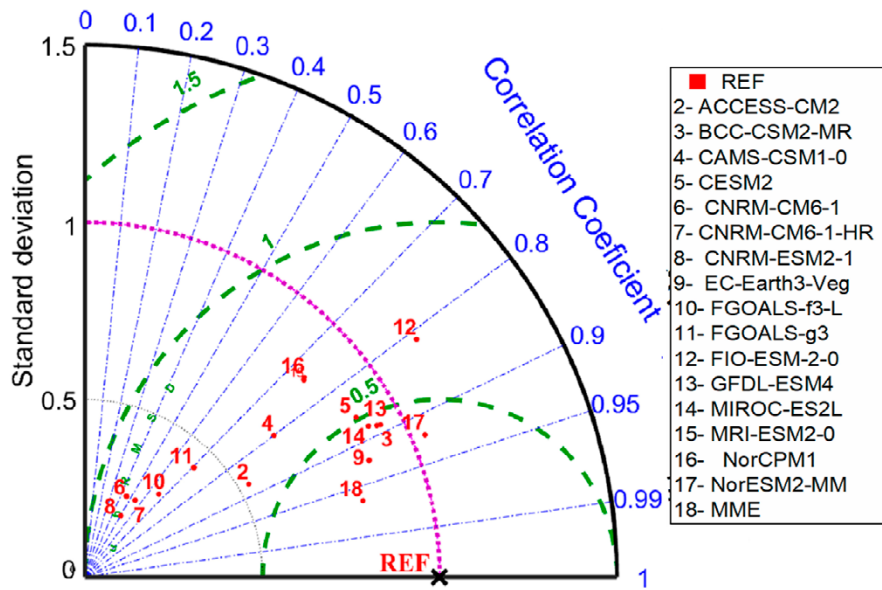


Figure 4. Comparison of annual GCMs-CMIP6 models against satellite-based rainfall CHIRPS from 1985 to 2014

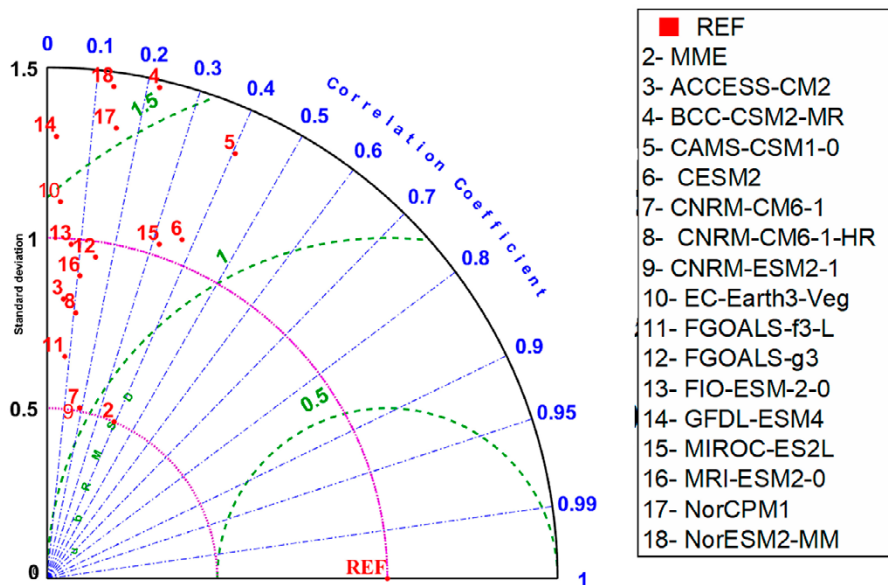


Figure 5. Comparison of GCMs-CMIP6 summer monsoon rain against CHIRPS from 1985 to 2014.

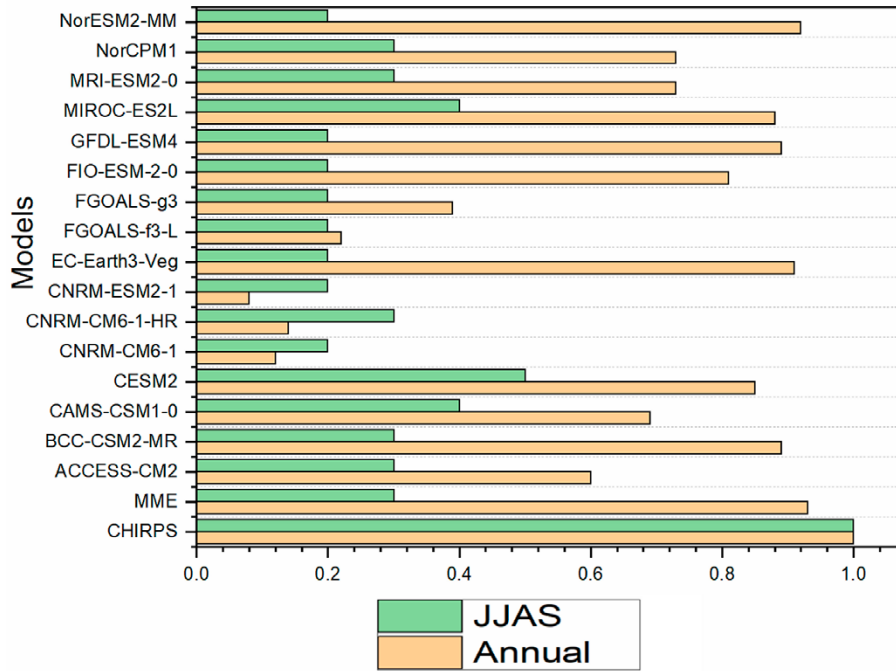


Figure 6. Summarizing Taylor Skill Score (TSS) of Annual

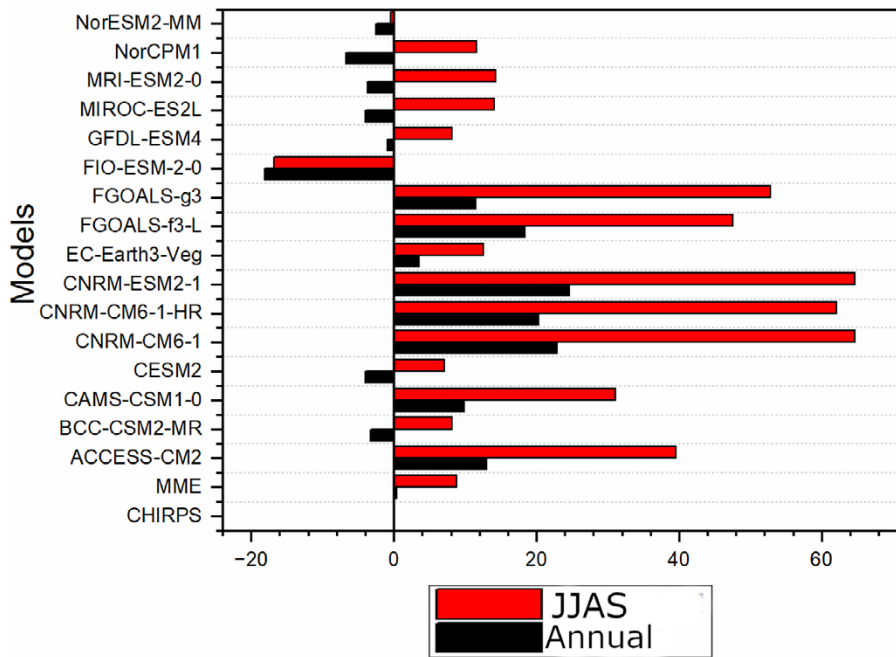


Figure 7. Bias for annual and JJAS multi-model ensemble and CHIRPS

other CIMP6 models in all statistical tests during the annual comparison. More so, NorESM2-MM demonstrated the highest CC with reference data, the largest TSS and SDV, and the lowest MAE and BIAS amongst the different CIMP6 models. As a result, it might be concluded that the six aforementioned models are more efficient than the other 16 GCMs in simulating annual rainfall across Sudan. It also found that the CNRM-ESM2-1, CNRM-CM6-1, CNRM-CM6-1-HR, and FGOALS-f3-L produced a much

larger bias and significantly lower TSS and CC than other GCMs. In particular, CNRM-ESM2-1 exhibited the lowest CC (0.08), the largest bias of 24.65 annually, and 64.66 in JJAS. Consequently, these four models are considered incapable of simulating rainfall over Sudan since they have produced statistically insignificant results. Other remaining models (including FIO-ESM-2-0, MRI-ESM2-0, ACCESS-CM2, and FGOALS-g3) displayed varied scores among different statistical tests.

Table 2. Summary of statistical that presents the findings of comparisons among annual using CHIRPS Rainfall data and historical simulation multi-Model data

Models	TSS	CC	SDV	BIAS	MAE	RMSD
CHIRPS	1.00	1.00	1.00	0.00	0.00	0.00
MME	0.93	0.96	0.81	0.42	6.76	10.37
ACCESS-CM2	0.60	0.87	0.53	12.96	14.90	24.13
BCC-CSM2-MR	0.89	0.89	0.94	-3.24	11.01	15.98
CAMS-CSM1-0	0.69	0.80	0.66	9.86	14.53	23.11
CESM2	0.85	0.86	0.89	-3.95	11.81	17.72
CNRM-CM6-1	0.12	0.46	0.26	22.93	24.69	38.57
CNRM-CM6-1-HR	0.14	0.55	0.26	20.28	23.01	36.31
CNRM-ESM2-1	0.08	0.50	0.20	24.65	25.92	39.71
EC-Earth3-Veg	0.91	0.93	0.87	3.54	9.06	13.53
FGOALS-f3-L	0.22	0.66	0.31	18.35	21.37	33.54
FGOALS-g3	0.39	0.71	0.43	11.49	17.65	28.24
FIO-ESM-2-0	0.81	0.81	1.15	-18.12	20.77	29.18
GFDL-ESM4	0.89	0.89	0.93	-0.85	9.82	15.73
MIROC-ES2L	0.88	0.88	0.91	-4.00	11.45	16.48
MRI-ESM2-0	0.73	0.74	0.83	-3.64	16.69	23.24
NorCPM1	0.73	0.74	0.84	-6.66	17.74	24.05
NorESM2-MM	0.92	0.92	1.04	-2.54	8.58	13.91

Table 3. Summary of statistical that presents the findings of comparisons among JJAS using CHIRPS Rainfall data and historical simulation multi-model data

Models	TSS	CC	SDV	BIAS	MAE	RMSD
CHIRPS	1.0	1.00	1	0.00	0.00	0.00
MME	0.3	0.39	0.50	8.80	9.16	10.78
ACCESS-CM2	0.3	0.06	0.82	39.55	39.55	40.45
BCC-CSM2-MR	0.3	0.22	1.48	8.16	11.18	13.45
CAMS-CSM1-0	0.4	0.41	1.36	31.06	31.06	32.31
CESM2	0.5	0.37	1.07	7.04	8.88	10.53
CNRM-CM6-1	0.2	0.19	0.51	64.66	64.66	65.04
CNRM-CM6-1-HR	0.3	0.11	0.78	62.11	62.11	62.63
CNRM-ESM2-1	0.2	0.19	0.51	64.66	64.66	65.04
EC-Earth3-Veg	0.2	-0.04	1.11	12.53	13.06	16.17
FGOALS-f3-L	0.2	0.08	0.65	47.51	47.51	48.14
FGOALS-g3	0.2	-0.15	0.95	52.78	52.78	53.71
FIO-ESM-2-0	0.2	-0.07	0.98	-16.79	17.49	19.43
GFDL-ESM4	0.2	0.02	1.30	8.11	10.93	13.60
MIROC-ES2L	0.4	0.32	1.03	14.04	14.19	16.16
MRI-ESM2-0	0.3	0.11	0.89	14.30	14.54	16.66
NorCPM1	0.3	0.15	1.34	11.60	13.11	15.58
NorESM2-MM	0.2	-0.13	1.46	-0.42	10.09	12.63

Spatial annual and JJAS mean evaluation of rainfall simulations

Sudan has a wide variety of rainfall variations. Hence, it is necessary to understand the fluctuations of rainfall across the entire parts of our study area. In this section, the spatial distribution of simulated precipitation from 16 GCMs as well as MME was assessed versus the CHIRPS dataset on the annual and seasonal (JJAS) cycle during 1985-2014, as illustrated in Figures 8 and 9. Our initial focus was on how well the GCMs could recreate the observed spatial variability of precipitation along the study domain. Both annual and intra-annual results show that most of the CMIP6 models can replicate the orographic precipitation pattern concerning the CHIRPS dataset. Moreover, the behavior of all CMIP6 models runs against the reference dataset demonstrating that rainfall increases towards the South. Nevertheless, some discrepancies exist among the different GCMs from 1985 to 2014. The average maximum and lowest annual precipitation were between (5-120 mm), respectively, and JJAS’s mean maximum was more than

120mm and the lowest was greater than 5 mm. The mean maximum value was observed over the south to the south-east zones across all models, whilst the mean lowest value was detected over the Northern parts. The results in Figures 8 and 9 further revealed that the MME model tends to follow the reference data; however, certain variations in the amount of precipitation were observed in comparison to the CHIRPS dataset. The following eight products: BCC-CSM2-MR, CAMS-CSM1-0, CESM2, EC-Earth3-Veg, GFDL-ESM4, MIROC-ES2L, MRI-ESM2-0, and NorESM2-MM were shown to be efficient in simulating the spatial change of precipitation based on the reference dataset. However, they have slight overestimate or underestimate spatial mean distribution (2-120mm/month) relative to the other models. In particular, NorESM2-MM performs better than other GGMs and exhibits lesser bias through the annual and seasonal phases.

On the other hand, other superior seven GGMs exhibited slight variations of distribution rainfall in comparison to the reference dataset. For example, CAMS-CSM1-0

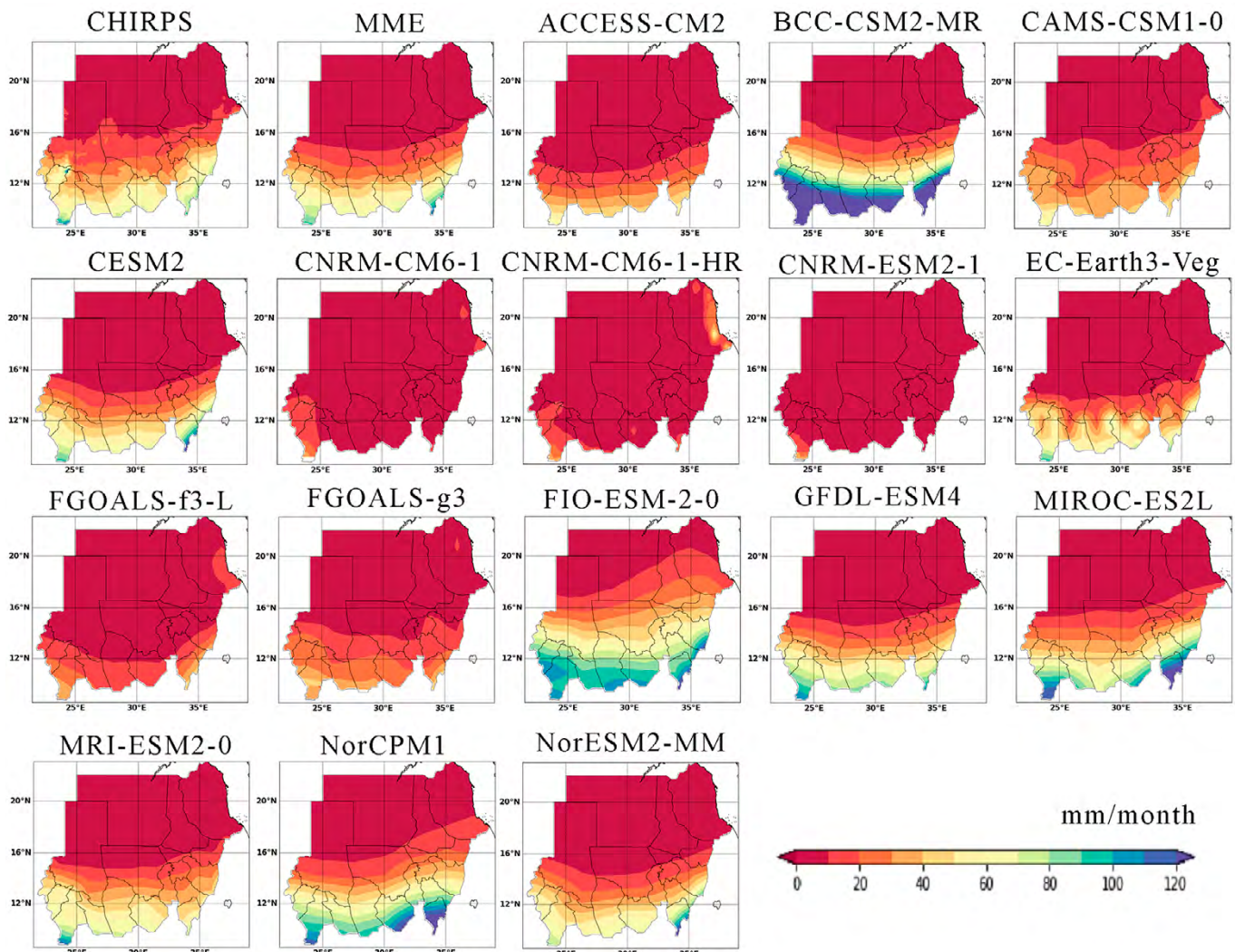


Figure 8. Spatial patterns of annual mean rainfall observation dataset and data simulation from (1985-2014)

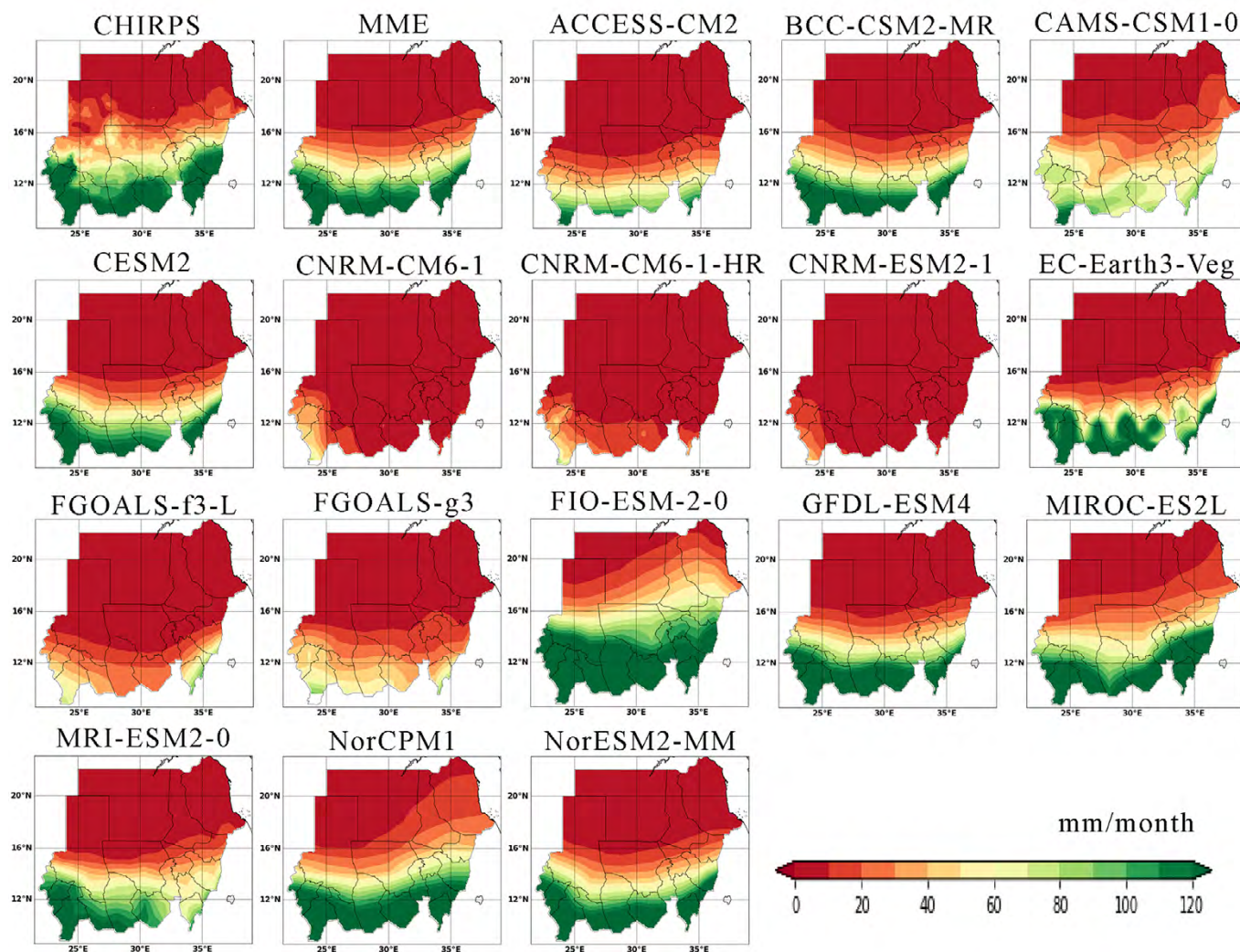


Figure 9. Spatial patterns of JJAS mean rainfall observation and data simulation from (1985-2014)

reveals a shallow decrease in the precipitation magnitude over the Southern parts and a slight increase across the far Northeast parts; MIROC-ES2L and GFDL-ESM4, and BCC-CSM2-MR showed a certain increase in the rainfall along the Southern zones through the annual phase; EC-Earth3-Veg has a slight variation over the Southern, Southeastern, and Western borders; and MRI-ESM2-0 shows a decrease in the precipitation over the Southeast areas. It also observed that the subsequent products (including CNRM-CM6-1, CNRM-CM6-1-HR, CNRM-ESM2-1, FGOALS-f3-L) substantially underestimate the values of annual and seasonal rainfall over the majority of our study domain. Besides, FIO-ESM-2-0 and NorCPM1 appear to overestimate the rainfall over the far Northeast borders, as seen in Figures 8 and 9.

Spatial Distribution of the Bias

Analyzing the bias of GCMs products is crucial to determine the performance of GCMs simulations. In this part, we analyzed the spatial bias of 16 GCMs models and MME

at JJAS and yearly scale for the period of 1985-2014 over Sudan. However, such analysis will demonstrate how well the GCM can simulate the precipitation patterns over Sudan during the analyzed period. The spatial biases of the GCMs were determined as mean differences between those models' outputs and the respective CHIRPS precipitation during the annual and seasonal phases (see Figures 10 and 11). It found that, during the annual and seasonal (JJAS) phase, the bias over most areas for different models was between (+40) and (-40) mm (see Figures 10 and 11). Furthermore, MME exhibited the lowest amount of bias amongst all models, however, it slightly overestimated bias across the study area. The subsequent GCMs: MIROC-ES2L, NorESM2-MM, EC-Earth3-Veg, and GFDL-ESM4 showed analogous bias distribution with a relatively little bias (i.e. the amount of bias positive or negative is little than other models) over most areas in the country. Other models (including ACCESS-CM2, BCC-CSM2-MR, CAMS-CSM1-0, CESM2, CNRM-CM6-1, CNRM-CM6-1-HR, CNRM-ESM2-1, FGOALS-f3-L, FGOALS-g3) are con-

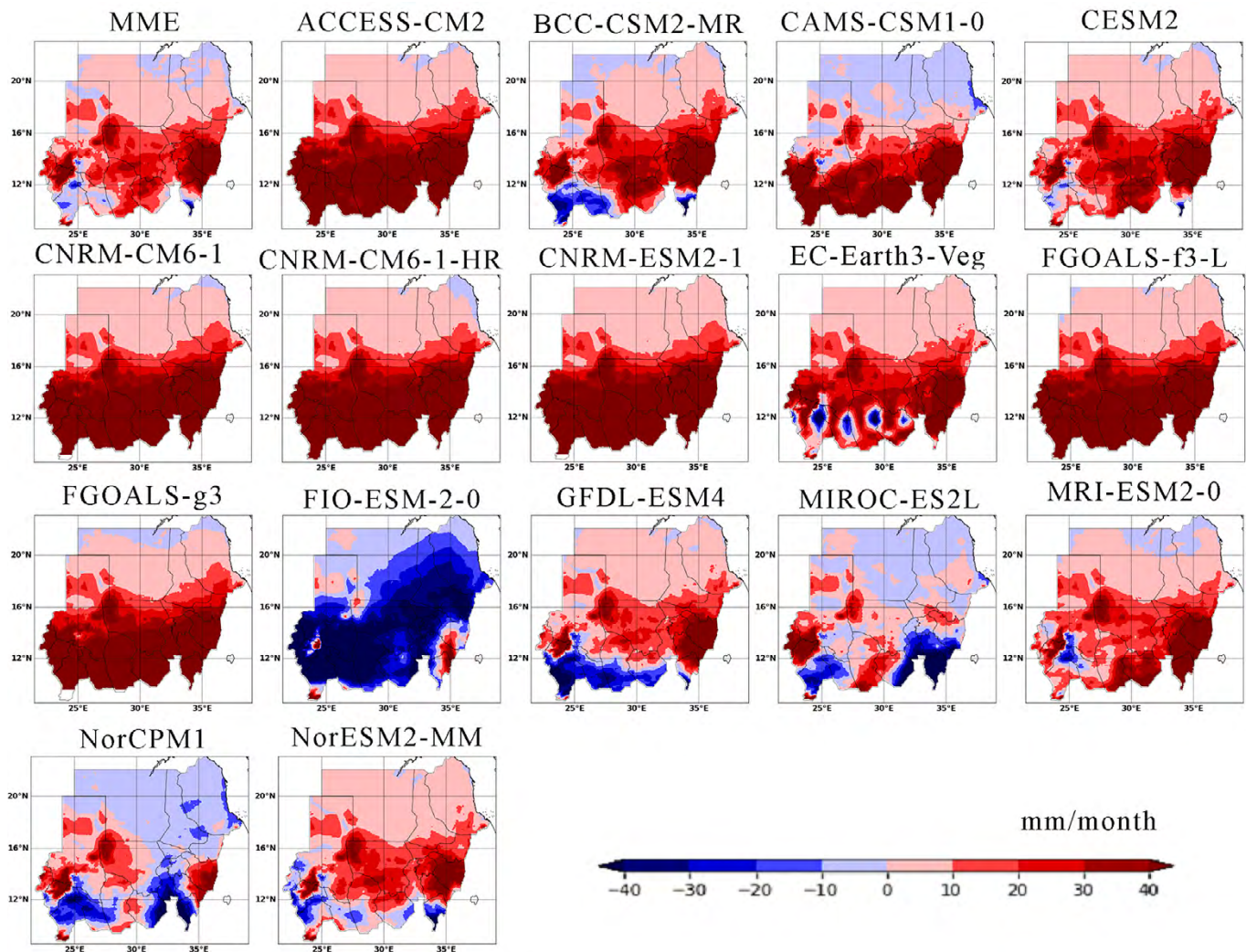


Figure 10. Bias of mean JJAS rainfall(mm/month) over Sudan based on CHIRPS Dataset 1985-2014

sistently overestimated bias based on CHIRPS data. Overall, MIROC-ES2L and NorESM2-MM displayed the lowest biases and showed better performance than other individual GCMs during the annual and JJAS rainfall. Based on the achieved results from Figures 10 and 11 it can be concluded that the considered CIMP6 GCMs for this study are not able to simulate precipitation patterns accurately over the region. The findings of this analysis could be of great use in identifying potential improvements in the GCMs and optimizing the model's parameters for future predictions.

Delta Bias Correction

We conducted a more in-depth analysis in this study to determine the extent to which the correction algorithm enhances the accuracy of the simulation models. The GCMs models are complex systems that simulate the Earth's climate system by solving a set of mathematical equations. It provides a representation of how the climate system might change due to natural variability, human activity, or

a combination of both. These models simulate the complex interactions of different elements of the climate system and land-sea-atmosphere-cryosphere interaction. However, these models are not perfect and can contain errors or biases. Therefore, corrections are necessary to improve the accuracy of the simulations, as these errors can lead to inaccurate projections of future weather conditions. In this work, to improve the accuracy of GCM simulations, we used the Delta method to correct the models.

Spatial bias distributions after correction of eight GCM models, in addition to MME, are shown in Figures 12 and 13. The correction is applied at each grid point across the spatial domain. After the correction, these models were evaluated against CHIRPS datasets as a reference from 1985 to 2014, on a seasonal (JJAS) and annual basis. The GCMs rainfall estimates are expected to be closer to the observed rainfall values after applying the correction. The obtained results in Figures 12 and 13 indicate that the spatial mean bias of GCMs precipitation has significantly (i.e. 0.2-6 mm/month overestimate or underestimate) re-

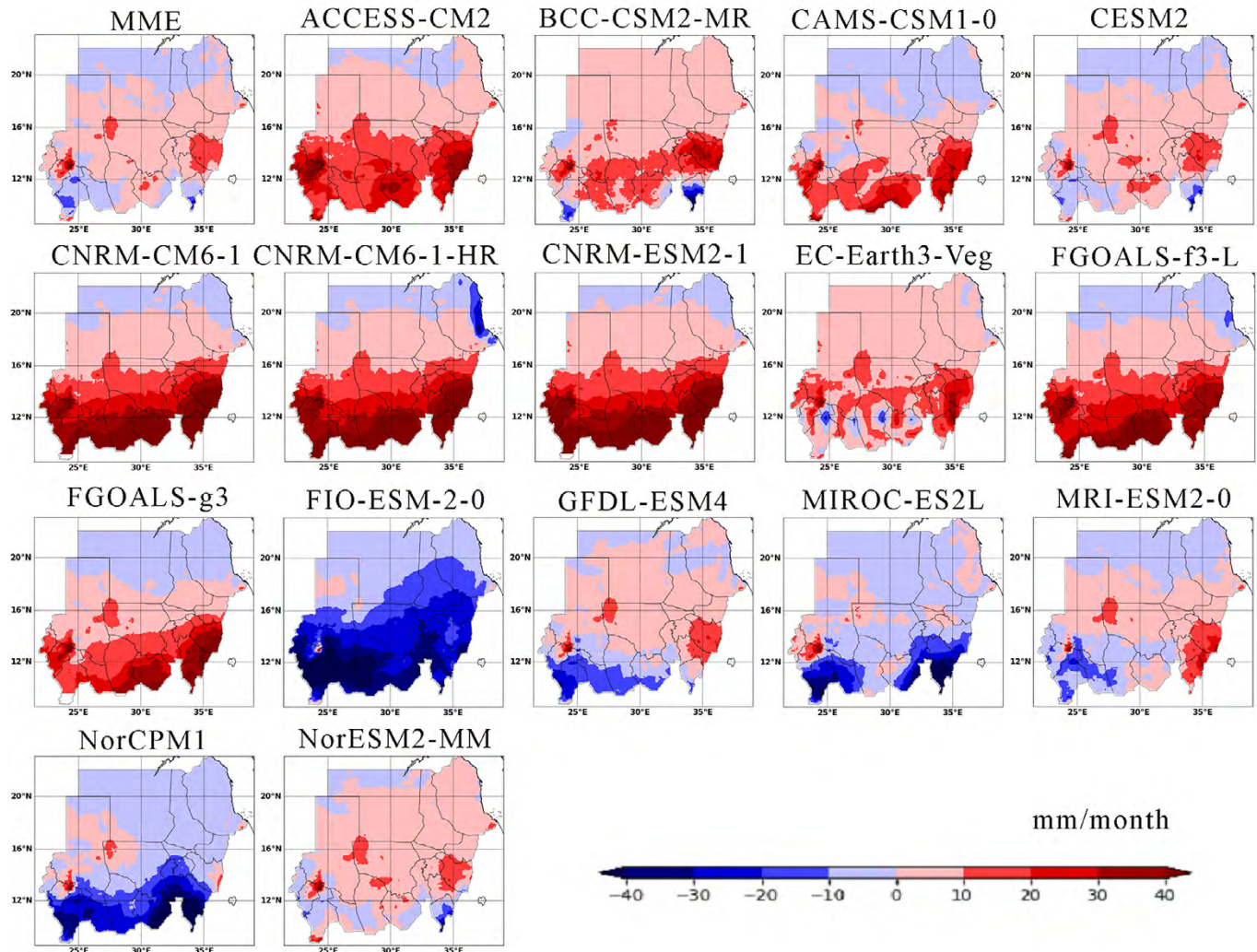


Figure 11. Bias of mean annual rainfall (mm/month) over Sudan based on CHIRPS Dataset 1985-2014

duced after applying the correction in comparison to the CHIRPS dataset. In addition, the reduction in the positive bias of the GCM estimates was more noticeable than the negative bias. MME and MIROC-ES2L demonstrate the lowest bias amount based on CHIRPS data, more so, they show better performance on the annual and seasonal (JJAS) scale after applying the correction in comparison to other GCMs. For most GCMs, greater improvement in the model's performance was observed through the annual rainfall than the seasonal (JJAS) rainfall; however, only EC-Earth3-Veg showed a poor improvement of 3% over the original. Although BCC-CSM2-MR has reduced the bias amount after applying the correction; nevertheless,

it enlarged the bias domain over the study area, which cannot be ignored and might result in more uncertainties in the future projection. The model's ensemble mean has proved its ability to be trusted for any further analysis regarding future projections among the annual and seasonal phases, according to their shown performance against the observations. Overall, the spatial mean bias correction of GCMs rainfall distribution using the CHIRPS dataset is an effective method for improving the accuracy of GCM precipitation estimates. However, it is important to note that the correction is not perfect and should be used with caution, especially in regions with complex precipitation patterns.

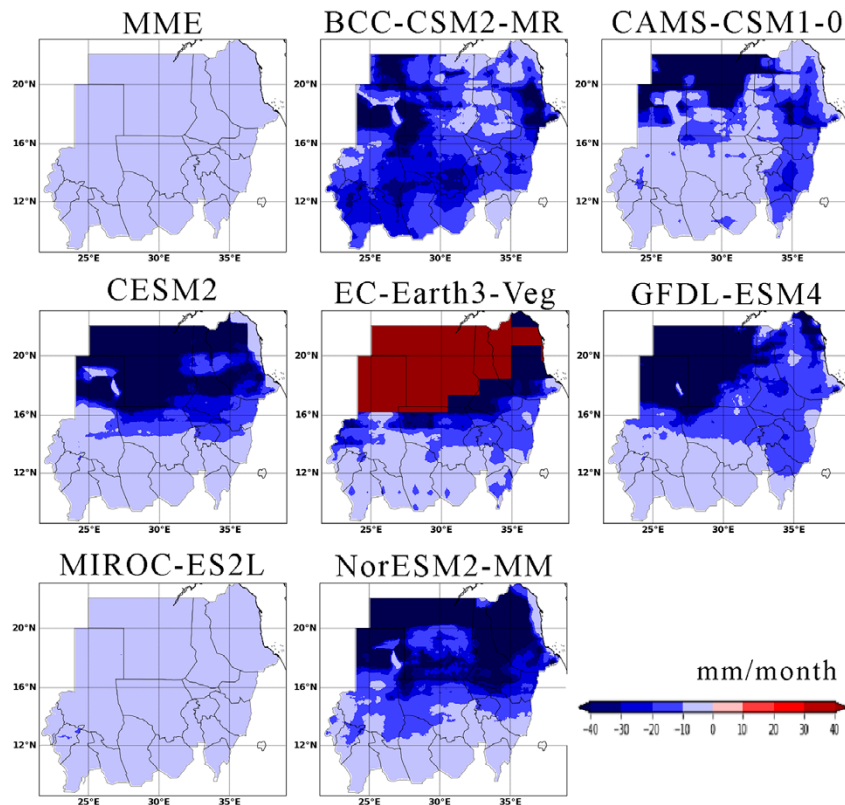


Figure 12. Spatial pattern of Bias after correction JJAS Rainfall period 1985–2014 based on CHIRPS dataset

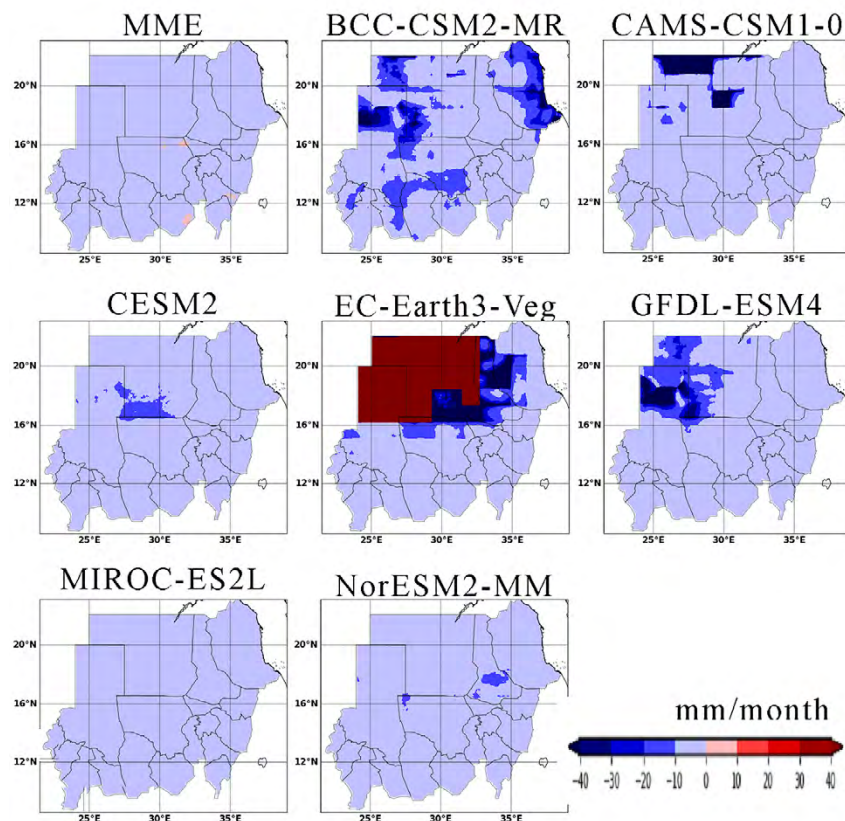


Figure 13. Spatial pattern of Bias after correction of annual rainfall from 1985–2014 based on the CHIRPS dataset

Discussion

Climate models, such as those included in the Coupled Model Intercomparison Project Phase 6 (CMIP6), are critical tools in understanding and projecting future climate change. These models simulate the most complex aspects of the climate system, including rainfall, sea level, temperature, and ocean circulation, and are used to inform policymakers, as well as businesses and individuals, about the expected impacts of climate change. One of crucial regions that requires accurate evaluation of climate models is the study domain, is the study domain highly vulnerable to the impacts of climate change. Climate models need to simulate rainfall patterns correctly to aid decision-makers in developing strategies to mitigate the effects of climate change on agriculture and other activities. This study used high-resolution satellite-based precipitation with Station (CHIRPS.v2) monthly precipitation datasets with a $0.05^\circ \times 0.05^\circ$ spatial resolution (Babaousmail et al., 2019; Ngoma et al., 2021). While previous studies on this domain, used source observation data over Sudan and employed CRU TS as reference data, they examine the changes in monsoon's (June–September) future precipitation over three zones distributed through Sudan based on GCMs from CMIP5 and (CMIP6). The models are GISS-E2-H, IPSL- CM5A-MR, and MPI-ESM-LR (BCC-CSM2-MR, INM-CM4-9 MPI-ESM1-2-LR) in addition to the ensemble mean of each group Given systematic errors in the GCMs simulations (Hamadalnel et al., 2022). Therefore, in this study, we focused on the evaluation and correction analysis of the regional rainfall simulation of the CMIP6 model over Sudan, considering the rainfall pattern, evaluation of the rainfall simulation, spatial distribution of bias, and bias correction. Before evaluating rainfall simulations, it is essential first to understand the observed rainfall pattern to ensure the accuracy of the results. Sudan's rainfall pattern is primarily influenced by the African monsoon system, which is responsible for most of the country's annual precipitation and seasonal (JJAS) from June to September. Observations of rainfall patterns in Sudan showed that

the distribution of rainfall varies significantly across the region. The Southern region received the highest amount of rainfall of 120 mm (Figures 8 and 9), while the Northern part received the least.

Sudan also experiences rainfall variability, which is attributed to the large-scale circulation patterns, such as the Inter-Tropical Convergence Zone (ITCZ) and the El-Nino Southern Oscillation (ENSO) (Alriah et al., 2021). In this study, the evaluation was conducted based on metrics such as the correlation coefficient (R), RMSE, and the Taylor diagram, which provides a graphical representation of the accuracy of the simulated rainfall pattern. The results of the evaluation showed that most of the employed CMIP6 models for this study accurately simulated the rainfall pattern over Sudan in annual and seasonal, but with a positive bias in most parts of Sudan, particularly in the Northwestern part of the country.

The Coupled Model Intercomparing Project (CMIP), which is at the cutting edge of exploring the depth of the planet's past, present, and future climate, has emerged as a key tool in climate science, providing the scientific communities with crucial data for research that informs important assessment activities like the ongoing IPCC process and other fields (Taylor et al., 2012). An assessment of the simulated findings of these GCMs versus the observation must be completed before taking a prospective look at potential future changes, particularly on a regional scale. In most cases, this process is carried out by comparing the simulations to the observations (Trigo & Palutikof, 2001), since it guarantees that the models can accurately represent some aspects of the climate system while employing model performance indicators to assess their potential and limitations (Gleckler et al., 2008). Consequently, the projection process is possible. The results of this study highlight the importance of evaluating and correcting biases in climate models to provide accurate information for future studies of climate change projection.

Conclusion

The study presents the evaluation and performance of 16 GCMs-CMIP6 models and compares their ability to accurately replicate observational satellite-based data over Sudan between 1985 and 2014. After conducting comprehensive statistical error measurements of the GCMs models' products over Sudan including Pearson Correlation Coefficient, Standard Deviation, Taylor Skill Score, Mean Absolute Error, absolute bias (BIAS), and, normalized mean root square error, we found that:

1. MME, which averaged the better GCMs models, demonstrated the strongest overall performance.

Additionally, three individual models – NorESM2-MM, MIROC-ES2L, and BCC-CSM2-MR – proved relative accuracy (-12 to 12 mm of mean bias before correction) in reproducing both annual and seasonal patterns. However, several models, including ACCESS-CM2, FGOALS-f3-L, FGOALS-g3, CNRM-CM6-1, CNRM-CM6-1-HR, CNRM-ESM2-1, and CNRM-ESM2-1, performed poorly in simulating the observed data.

2. The models improved by 0-18% over the origin progress after applying bias correction (Delta method),

especially the ensemble mean (MME). In contrast, some CMIP6 models had slight deviations from the observations.

Generally, the study suggests that the MME and the three individual models offer the most promising options for future modeling efforts and have a satisfactory performance after correction.

Author declaration: All authors declare that: there is no conflict of interest.

Reference

- Ahmed, N., & Elhag, M. M. (2011). Major climate indicators of ongoing drought in Sudan. *Journal of Hydrology*, 409(3–4), 612–625. <https://doi.org/10.1016/j.jhydrol.2011.08.047>
- Akurut, M., Willems, P., & Niwagaba, C. B. (2014). Potential impacts of climate change on precipitation over lake Victoria, East Africa, in the 21st century. *Water*, 6(9), 2634–2659. <https://doi.org/10.3390/w6092634>
- Alhuseen, A. (2014). *Analysis of policy network of adapting to climate change in Sudan*. 4(11), 1–4. <https://www.ijsrp.org/research-paper-1114.php?rp=P353366>
- Almazroui, M., Saeed, F., Saeed, S., Nazrul Islam, M., Ismail, M., Klutse, N. A. B., & Siddiqui, M. H. (2020). Projected Change in Temperature and Precipitation Over Africa from CMIP6. *Earth Systems and Environment*, 4(3), 455–475. <https://doi.org/10.1007/s41748-020-00161-x>
- Alriah, M. A. A., Bi, S., Nkunuzimana, A., Elameen, A. M., Sarfo, I., & Ayugi, B. (2022). Multiple gridded-based precipitation products' performance in Sudan's different topographical features and the influence of the Atlantic Multidecadal Oscillation on rainfall variability in recent decades. *International Journal of Climatology*, 1–28. <https://doi.org/10.1002/joc.7845>
- Alriah, M. A. A., Bi, S., Shahid, S., Nkunuzimana, A., Ayugi, B., Ali, A., Bilal, M., Teshome, A., Sarfo, I., & Elameen, A. M. (2021). Summer monsoon rainfall variations and its association with atmospheric circulations over Sudan. *Journal of Atmospheric and Solar-Terrestrial Physics*, 225, 105751. <https://doi.org/10.1016/j.jastp.2021.105751>
- Babaousmail, H., Hou, R., Ayugi, B., & Gnitou, G. T. (2019). Evaluation of satellite-based precipitation estimates over Algeria during 1998–2016. *Journal of Atmospheric and Solar-Terrestrial Physics*, 195, 105139. <https://doi.org/10.1016/j.jastp.2019.105139>
- Babaousmail, H., Hou, R., Ayugi, B., Ojara, M., Ngoma, H., Karim, R., Rajasekar, A., & Ongoma, V. (2021). Evaluation of the performance of cmip6 models in reproducing rainfall patterns over north africa. *Atmosphere*, 12(4), 1–25. <https://doi.org/10.3390/atmos12040475>
- Babaousmail, H., Hou, R., Ayugi, B., Sian, K. T. C. L. K., Ojara, M., Mumo, R., Chehbouni, A., & Ongoma, V. (2022). Future changes in mean and extreme precipitation over the Mediterranean and Sahara regions using bias-corrected CMIP6 models. *International Journal of Climatology*, 42(14), 7280–7297. <https://doi.org/10.1002/joc.7644>
- Badr, H. S., Dezfuli, A. K., Zaitchik, B. F., & Peters-Lidard, C. D. (2016). Regionalizing Africa: Patterns of precipitation variability in observations and global climate models. *Journal of Climate*, 29(24), 9027–9043. <https://doi.org/10.1175/JCLI-D-16-0182.1>
- Bao, Y., Song, Z., & Qiao, F. (2020). FIO-ESM Version 2.0: Model Description and Evaluation. *Journal of Geophysical Research: Oceans*, 125(6), 1–21. <https://doi.org/10.1029/2019JC016036>
- Bethke, I., Wang, Y., Counillon, F., Keenlyside, N., Kimmritz, M., Fransner, F., Samuelsen, A., Langehaug, H., Svendsen, L., Chiu, P. G., Passos, L., Bentsen, M., Guo, C., Gupta, A., Tjiputra, J., Kirkevåg, A., Olivié, Di., Seland, Ø., Solsvik Vågane, J., Fan, Y., & Eldevik, T. (2021). NorCPM1 and its contribution to CMIP6 DCP. *Geoscientific Model Development*, 14(11), 7073–7116. <https://doi.org/10.5194/gmd-14-7073-2021>
- Collins, M., & Senior, C. A. (2002). Projections of future climate change. *Weather*, 57(8), 283–287. <https://doi.org/10.1256/004316502320517371>
- El Gamri, T., Saeed, A. B., & Abdalla, A. (2021). Rainfall of the Sudan: Characteristics and Prediction. *Journal of Faculty of Arts, University of Khartoum*, 27. <https://doi.org/10.53332/jfa.v27i.624>
- Elramlawi, H. R., Mohammed, H. I., Elamin, A. W., Abdallah, O. A., & Taha, A. A. A. M. (2019). Adaptation of sorghum (*Sorghum bicolor* L. Moench) crop yield to climate change in eastern dryland of Sudan. *Handbook of Climate Change Resilience; Springer: Cham, Switzerland*, 2549–2573. <https://doi.org/10.1007/978-3-319-71025-9>
- Expósito, F. J., González, A., Pérez, J. C., Díaz, J. P., & Taima, D. (2015). High-resolution future projections of temperature and precipitation in the Canary Islands. *Journal of Climate*, 28(19), 7846–7856.
- Gleckler, P. J., Taylor, K. E., & Doutriaux, C. (2008). Performance metrics for climate models. *Journal of Geophysical Research Atmospheres*, 113(6), 1–20. <https://doi.org/10.1029/2007JD008972>
- Hajima, T., Watanabe, M., Yamamoto, A., Tatebe, H., Noguchi, M. A., Abe, M., Ohgaito, R., Ito, A., Yamazaki, D., Okajima, H., Ito, A., Takata, K., Ogochi, K., Watanabe, S., & Kawamiya, M. (2020). Development of

- the MIROC-ES2L Earth system model and the evaluation of biogeochemical processes and feedbacks. *Geoscientific Model Development*, 13(5), 2197–2244. <https://doi.org/10.5194/gmd-13-2197-2020>
- Hamadanel, M., Zhu, Z., Gaber, A., Iyakaremye, V., & Ayugi, B. (2022). Possible changes in Sudan's future precipitation under the high and medium emission scenarios based on bias adjusted GCMs. *Atmospheric Research*, 269, 106036. <https://doi.org/10.1016/j.atmosres.2022.106036>
- Hemanandhini, S., & Vignesh, R. L. (2023). Performance evaluation of CMIP6 climate models for selecting a suitable GCM for future precipitation at different places of Tamil Nadu. *Environmental Monitoring and Assessment*, 195(8), 928–928. <https://doi.org/10.1007/s10661-023-11454-9>
- Ishida, K., Ercan, A., Trinh, T., Jang, S., Kavvas, M. L., Ohara, N., Chen, Z. Q., Kure, S., & Dib, A. (2020). Trend analysis of watershed-scale annual and seasonal precipitation in Northern California based on dynamically downscaled future climate projections. *Journal of Water and Climate Change*, 11(1), 86–105. <https://doi.org/10.2166/wcc.2018.241>
- Karim, R., Tan, G., Ayugi, B., Shahzaman, M., Babaousmail, H., Ngoma, H., & Ongoma, V. (2023). Projected changes in surface air temperature over Pakistan under bias-constrained CMIP6 models. *Arabian Journal of Geosciences*, 16(3), 205. <https://doi.org/10.1007/s12517-023-11243-1>
- Kawai, H., Yukimoto, S., Koshiro, T., Oshima, N., Tanaka, T., Yoshimura, H., & Nagasawa, R. (2019). Significant improvement of cloud representation in the global climate model MRI-ESM2. *Geoscientific Model Development*, 12(7), 2875–2897. <https://doi.org/10.5194/gmd-12-2875-2019>
- Klutse, N. A. B., Quagraine, K. A., Nkrumah, F., Quagraine, K. T., Berkoh-Oforiwa, R., Dzrobi, J. F., & Sylla, M. B. (2021). The Climatic Analysis of Summer Monsoon Extreme Precipitation Events over West Africa in CMIP6 Simulations. *Earth Systems and Environment*, 5(1), 25–41. <https://doi.org/10.1007/s41748-021-00203-y>
- Kumar, P., Wiltshire, A., Mathison, C., Asharaf, S., Ahrens, B., Lucas-Picher, P., Christensen, J. H., Gobiet, A., Saeed, F., Hagemann, S., & Jacob, D. (2013). Downscaled climate change projections with uncertainty assessment over India using a high resolution multi-model approach. *Science of the Total Environment*, 468, S18–S30. <https://doi.org/10.1016/j.scitotenv.2013.01.051>
- Maroneze, M. M., Zepka, L. Q., Vieira, J. G., Queiroz, M. I., & Jacob-Lopes, E. (2014). The primary tools of the analyses targeted at determining what climate we are likely to have in the near and not-so-near future use dynamical downscaling with Regional Climate Models (RCMs) and Global Climate Models (GCMs). *Revista Ambiente e Agua*, 9(3), 445–458. <https://doi.org/10.4136/1980-993X>
- Meehl, G. A., Arblaster, J. M., Bates, S., Richter, J. H., Tebaldi, C., Gettelman, A., Medeiros, B., Bacmeister, J., DeRepentigny, P., Rosenbloom, N., Shields, C., Hu, A., Teng, H., Mills, M. J., & Strand, G. (2020). Characteristics of Future Warmer Base States in CESM2. *Earth and Space Science*, 7(9). <https://doi.org/10.1029/2020EA001296>
- Mendez, M., Maathuis, B., Hein-Griggs, D., & Alvarado-Gamboa, L. F. (2020). Performance evaluation of bias correction methods for climate change monthly precipitation projections over Costa Rica. *Water*, 12(2). <https://doi.org/10.3390/w12020482>
- Mkala, E. M., Mwanzia, V., Nzei, J., Oluoch, W. A., Ngarega, B. K., Wanga, V. O., Oulo, M. A., Munyao, F., Kilongo, F. M., Rono, P., Waswa, E. N., Mutinda, E. S., Ochieng, C. O., Mwachala, G., Hu, G. W., Wang, Q. F., Katunge, J. K., & Victoire, C. I. (2023). Predicting the potential impacts of climate change on the endangered endemic annonaceae species in east africa. *Heliyon*, 9(6), e17405. <https://doi.org/10.1016/j.heliyon.2023.e17405>
- Ngoma, H., Wen, W., Ojara, M., & Ayugi, B. (2021). Assessing current and future spatiotemporal precipitation variability and trends over Uganda, East Africa, based on CHIRPS and regional climate model datasets. *Meteorology and Atmospheric Physics*, 133(3), 823–843. <https://doi.org/10.1007/s00703-021-00784-3>
- Rajbhandari, R., Shrestha, A. B., Nepal, S., & Wahid, S. (2018). Projection of Future Precipitation and Temperature Change over the Transboundary Koshi River Basin Using Regional Climate Model PRECIS. *Atmospheric and Climate Sciences*, 08(02), 163–191. <https://doi.org/10.4236/acs.2018.82012>
- Rajbhandari, R., Shrestha, A. B., Nepal, S., & Wahid, S. (2018). Projection of future precipitation and temperature change over the transboundary Koshi River basin using regional climate model PRECIS. *Atmospheric and Climate Sciences*, 8(2), 163–191. <https://doi.org/10.4236/acs.2018.82012>
- Salih, A. A. M., Zhang, Q., & Tjernström, M. (2015). Lagrangian tracing of Sahelian Sudan moisture sources. *Journal of Geophysical Research*, 120(14), 6793–6808. <https://doi.org/10.1002/2015JD023238>
- Séférian, R., Nabat, P., Michou, M., Saint-Martin, D., Voltaire, A., Colin, J., Decharme, B., Delire, C., Berthet, S., Chevallier, M., Sénési, S., Franchisteguy, L., Vial, J., Mallet, M., Joetzjer, E., Geoffroy, O., Guérémy, J. F., Moine, M. P., Msadek, R., Ribes, A., Rocher, M., Roehrig, R., Salas-y-Méla, D., Sanchez, E., Terray, L., Valcke, S., Waldman, R., Aumont, O., Bopp, L., Deshayes, J., Éthé, C., & Madec, G. (2019). Evaluation of CNRM Earth System Model, CNRM-ESM2-1: Role of Earth System Processes in Present-Day and Future Climate. *Journal of Advances in Modeling Earth Systems*, 11(12), 4182–4227. <https://doi.org/10.1029/2019MS001791>

- Seland, Ø., Bentsen, M., Seland Graff, L., Olivié, D., Toniazzi, T., Gjermundsen, A., Debernard, J. B., Gupta, A. K., He, Y., Kirkevåg, A., Schwinger, J., Tjiputra, J., Schancke Aas, K., Bethke, I., Fan, Y., Griesfeller, J., Grini, A., Guo, C., Ilicak, M., ... Schulz, M. (2020). The Norwegian Earth System Model, NorESM2 – Evaluation of the CMIP6 DECK and historical simulations. *Geoscientific Model Development Discussions, February*, 1–68. <https://doi.org/10.5194/gmd-13-6165-2020>
- Siddig, K., Stepanyan, D., Wiebelt, M., Grethe, H., & Zhu, T. (2020). Climate change and agriculture in the Sudan: Impact pathways beyond changes in mean rainfall and temperature. *Ecological Economics*, 169, 106566. <https://doi.org/10.1016/j.ecolecon.2019.106566>
- Taylor, K. E., Stouffer, R. J., & Meehl, G. A. (2012). An overview of CMIP5 and the experiment design. *Bulletin of the American Meteorological Society*, 93(4), 485–498. <https://doi.org/10.1175/BAMS-D-11-00094.1>
- Tegegne, G., & Mellese, A. M. (2022). Multimodel ensemble projection of precipitation over South Korea using the reliability ensemble averaging. *Theoretical and Applied Climatology*, 1205–1214. <https://doi.org/10.1007/s00704-022-04350-8>
- Trigo, R. M., & Palutikof, J. P. (2001). Precipitation scenarios over Iberia: A comparison between direct GCM output and different downscaling techniques. *Journal of Climate*, 14(23), 4422–4446. [https://doi.org/10.1175/1520-0442\(2001\)014<4422:PSOAC>2.0.CO;2](https://doi.org/10.1175/1520-0442(2001)014<4422:PSOAC>2.0.CO;2)
- Voldoire, A., Saint-Martin, D., Sénési, S., Decharme, B., Alias, A., Chevallier, M., Colin, J., Guérémy, J. F., Michou, M., Moine, M. P., Nabat, P., Roehrig, R., Salas y Mélia, D., Séférian, R., Valcke, S., Beau, I., Belamari, S., Berthet, S., Cassou, C., ... Waldman, R. (2019). Evaluation of CMIP6 DECK Experiments With CNRM-CM6-1. *Journal of Advances in Modeling Earth Systems*, 11(7), 2177–2213. <https://doi.org/10.1029/2019MS001683>
- Walthall, C. L. . (2012). Climate Change and Agriculture in the US. *USDA Technical Bulletin 1935*, 186. <https://doi.org/10.1016/j.ecolecon.2019.106566>
- Wang, H., Li, L., Chen, X., & Wang, B. (2022). Evaluating the Nature and Extent of Changes to Climate Sensitivity Between FGOALS-g2 and FGOALS-g3. *Journal of Geophysical Research: Atmospheres*, 127(3), 1–19. <https://doi.org/10.1029/2021JD035852>
- Weijer, W., Cheng, W., Garuba, O. A., Hu, A., & Nadiga, B. T. (2020). CMIP6 Models Predict Significant 21st Century Decline of the Atlantic Meridional Overturning Circulation. *Geophysical Research Letters*, 47(12). <https://doi.org/10.1029/2019GL086075>
- Williams, M., & Nottage, J. (2006). Impact of extreme rainfall in the central Sudan during 1999 as a partial analogue for reconstructing early Holocene prehistoric environments. *Quaternary International*, 150(1), 82–94. <https://doi.org/10.1016/j.quaint.2006.01.009>
- Wu, T., Yu, R., Lu, Y., Jie, W., Fang, Y., Zhang, J., Zhang, L., Xin, X., Li, L., Wang, Z., Liu, Y., Zhang, F., Wu, F., Chu, M., Li, J., Li, W., Zhang, Y., Shi, X., Zhou, W., Yao, J., Liu, X., Zhao, H., Yan, J., Wei, M., Xue, W., Huang, A., Zhang, Y., Zhang, Y., Shu, Q., & Hu, A. (2021). BCC-CSM2-HR: A high-resolution version of the Beijing Climate Center Climate System Model. *Geoscientific Model Development*, 14(5), 2977–3006. <https://doi.org/10.5194/gmd-14-2977-2021>
- Zheng, X., Li, Q., Zhou, T., Tang, Q., Van Roekel, L. P., Golaz, J. C., Wang, H., & Cameron-Smith, P. (2022). Description of historical and future projection simulations by the global coupled E3SMv1.0 model as used in CMIP6. *Geoscientific Model Development*, 15(9), 3941–3967. <https://doi.org/10.5194/gmd-15-3941-2022>